Circulating glucose levels modulate neural control of desire for high-calorie foods in humans

Kathleen A. Page,[1,2] Dongju Seo,[3] Renata Belfort-DeAguiar,[1] Cheryl Lacadie,[4] James Dzuira,[5] Sarita Naik,[1] Suma Amarnath,[1] R. Todd Constable,[4] Robert S. Sherwin,[1] and Rajita Sinha[3]

[1]Section of Endocrinology, Yale University School of Medicine, New Haven, Connecticut, USA. [2]Division of Endocrinology, University of Southern California Keck School of Medicine, Los Angeles, California, USA. [3]Department of Psychiatry, [4]Department of Radiology, and [5]Yale Center for Clinical Investigation, Yale University School of Medicine, New Haven, Connecticut, USA.

Obesity is a worldwide epidemic resulting in part from the ubiquity of high-calorie foods and food images. Whether obese and nonobese individuals regulate their desire to consume high-calorie foods differently is not clear. We set out to investigate the hypothesis that circulating levels of glucose, the primary fuel source for the brain, influence brain regions that regulate the motivation to consume high-calorie foods. Using functional MRI (fMRI) combined with a stepped hyperinsulinemic euglycemic-hypoglycemic clamp and behavioral measures of interest in food, we have shown here that mild hypoglycemia preferentially activates limbic-striatal brain regions in response to food cues to produce a greater desire for high-calorie foods. In contrast, euglycemia preferentially activated the medial prefrontal cortex and resulted in less interest in food stimuli. Indeed, higher circulating glucose levels predicted greater medial prefrontal cortex activation, and this response was absent in obese subjects. These findings demonstrate that circulating glucose modulates neural stimulatory and inhibitory control over food motivation and suggest that this glucose-linked restraining influence is lost in obesity. Strategies that temper postprandial reductions in glucose levels might reduce the risk of overeating, particularly in environments inundated with visual cues of high-calorie foods.

Introduction

Glucose is an important regulatory signal and the primary fuel source for the brain (1). Specialized glucose-sensing neurons located in the hypothalamus, hindbrain, and forebrain are important in the control of glucose homeostasis and feeding behavior (1, 2). Transient declines in blood glucose increase hunger and therefore mobilize an individual toward food consumption (3, 4), particularly high-sugar (5) and high-fat foods (6). Further, hypoglycemia provokes a physiological stress response to mobilize the individual toward seeking food and restoring glucose levels (6). While the role of hindbrain and hypothalamic neuronal responses in hypoglycemia and maintaining energy homeostasis is well characterized (1, 2, 7), the specific neural mechanisms mediating the motivational drive for food under mild hypoglycemic conditions are not known. We hypothesized that a reduction in circulating glucose, to levels commonly observed several hours after glucose ingestion in healthy individuals (8), would activate brain reward and motivation pathways, including the striatum and insula, while concomitantly increasing desire for high-calorie foods.

To test this hypothesis, we performed functional MRI (fMRI) studies in 14 healthy (9 nonobese and 5 obese) subjects 2 hours after ingestion of a standardized lunch. Subjects viewed high-calorie food, low-calorie food, and non-food images while lying in the scanner during a stepped hyperinsulinemic euglycemic-hypoglycemic clamp. To control for potential session order effects, 7 additional subjects viewed the same pictures during a hyperinsulinemic euglycemic clamp under identical conditions (Figure 1A). Behavioral ratings of wanting and liking were presented after each food and non-food image (Figure 1B), and hunger ratings were assessed at the beginning and end of each phase. This approach allowed us to identify how a standardized reduction in circulating glucose, independent of changes in circulating insulin, interacts with external food cues to modulate the neural circuitry that controls feeding behavior.

Results

Metabolic changes

Plasma glucose was maintained at 88 ± 2 mg/dl during the euglycemic phase and reduced to 67 ± 1 mg/dl during the hypoglycemic phase of the study. Glucose levels were maintained at 92 ± 4 mg/dl throughout the euglycemic control study (Figure 2A). Plasma insulin levels were equivalent during both study sessions (Figure 2B). Plasma cortisol levels were significantly higher during the hypoglycemic versus the euglycemic phase ($P = 0.003$) but were not different throughout the euglycemic control study (Supplemental Figure 1; supplemental material available online with this article; doi:10.1172/JCI57873DS1). The mild hypoglycemic stimulus did not significantly alter plasma epinephrine, glucagon, leptin, or ghrelin levels. Growth hormone levels rose (hypoglycemic: 11.5 ± 1; euglycemic: 5.9 ± 2 ng/dl, $P < 0.001$) and C-peptide levels declined (hypoglycemic: 0.50 ± 0.07; euglycemic: 0.87 ± 0.1 ng/ml, $P < 0.001$) during the hypoglycemic versus the euglycemic phase, and they remained unchanged during the euglycemic control study.

Authorship note: Kathleen A. Page and Dongju Seo contributed equally to this work and serve as joint first authors. Rajita Sinha and Robert S. Sherwin contributed equally and serve as joint senior authors.

Conflict of interest: The authors have declared that no conflict of interest exists.

Citation for this article: *J Clin Invest.* 2011;121(10):4161–4169. doi:10.1172/JCI57873.

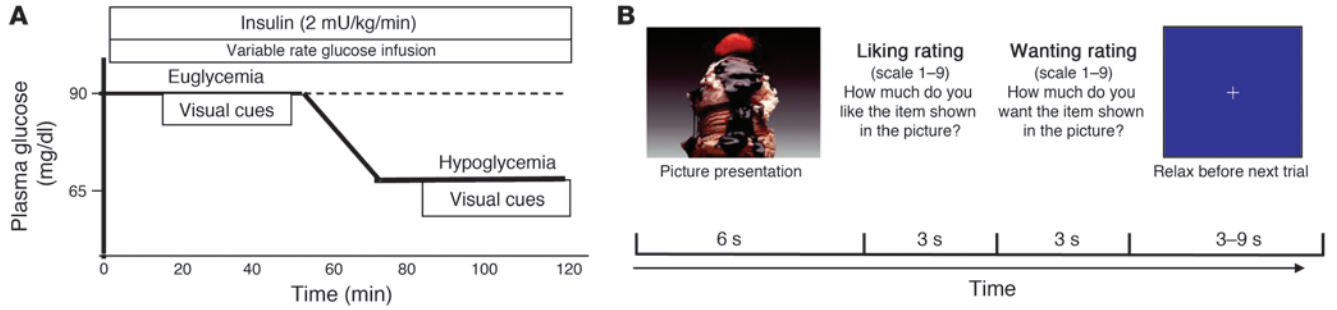

Figure 1
Study procedure. (**A**) While subjects were in the scanner, a hyperinsulinemic clamp was performed with a constant infusion of insulin along with variable amounts of glucose to maintain euglycemic conditions for the first 60 minutes. For the stepped clamp study (n = 14), plasma glucose was then lowered to approximately 65 mg/dl for the hypoglycemic phase. For the euglycemic control study (n = 7), plasma glucose was maintained at approximately 90 mg/dl (dotted line). During both conditions, functional scans were performed while subjects viewed images that were projected onto a screen in the scanner. (**B**) Time course of a single trial. Each trial consisted of 3 events. First, a high-calorie food, low-calorie food, or non-food picture appeared for 6 seconds. Second, two rating scales were presented for 3 seconds each and consisted of liking and wanting scales with values 1–9, where a rating of 1 indicated "not at all" and a rating of 9 indicated "very much." At the end of a trial, a fixation cross appeared, and subjects relaxed until the onset of the next trial.

Neural activation and behavioral ratings

Main effects of condition. In the total group, a significant effect was detected for euglycemic versus hypoglycemic conditions across all food and non-food visual stimuli (see Table 1 for all brain regions that were significantly affected by euglycemia relative to hypoglycemia). There was greater activation of the prefrontal cortex (PFC) and anterior cingulate cortex (ACC) under euglycemia relative to hypoglycemia, whereas the nucleus accumbens, insula, hypothalamus, thalamus, caudate, and putamen were preferentially activated under hypoglycemia relative to euglycemia (P < 0.05, corrected, covaried for BMI, Figure 3A). Hunger ratings were greater under hypoglycemic (5.7 ± 0.5) versus euglycemic (4.5 ± 0.5) conditions (P = 0.009) and did not significantly vary as a function of BMI. However, significant BMI group interactions were seen with condition. Obese individuals showed greater left substantia nigra/ventral tegmental area (SN/VTA) activation and greater bilateral activation of the hypothalamus, thalamus, striatum, and insula during hypoglycemia relative to euglycemia (P < 0.05, corrected). Furthermore, increased activation of the medial PFC or ACC under euglycemia relative to hypoglycemia did not occur in obese individuals (Figure 3B). Nonobese individuals demonstrated greater right insula and putamen activity during hypoglycemia relative to euglycemia and greater activity in the left SN/VTA, bilateral hippocampus, and medial PFC and ACC during euglycemia relative to hypoglycemia (Figure 3C).

Condition × task effects. Next we compared how the level of plasma glucose influenced the ability of visual food stimuli (high-calorie and low-calorie foods) to affect brain activation and wanting and liking of food (Figure 4). During euglycemia compared with hypoglycemia, there was significantly greater activation in the PFC and ACC, whereas hypoglycemia compared with euglycemia provoked greater activation in the insula and striatum in response to images of high- and low-calorie foods (P < 0.05, corrected, covaried for BMI, Figure 4A). Hypoglycemia compared with euglycemia also caused a greater wanting (P = 0.02, covaried for BMI) but no difference in liking of food (Figure 4B).

Mild hypoglycemia preferentially increased activation of the striatum and insula in response to high-calorie food stimuli (Figure 4C) and provoked a greater wanting (P = 0.006, covaried for BMI) but no difference in liking of high-calorie foods (Figure 4D). In contrast, low-calorie food cues did not provoke a differential brain response (data not shown) or a significant difference in the behavioral response to mild hypoglycemia compared with euglycemia (Supplemental Figure 2). These results could not be attributed to nonspecific time-related effects, since no differences in brain activation to food cues or in hunger ratings were observed during the second half of the euglycemic control study session compared with the first half (Supplemental Figure 3). Thus, mild hypoglycemia sets in motion adaptive mechanisms in motivational pathways to specifically increase wanting of high-energy and glucose-rich foods.

Neural activation and neuroendocrine correlations

The association of changes in circulating glucose and hormones with brain activation to high-calorie food images was assessed using whole-brain, voxel-based correlation analyses (Figure 5). Higher plasma glucose levels correlated with greater brain activity in executive control centers in the ACC and ventromedial PFC,

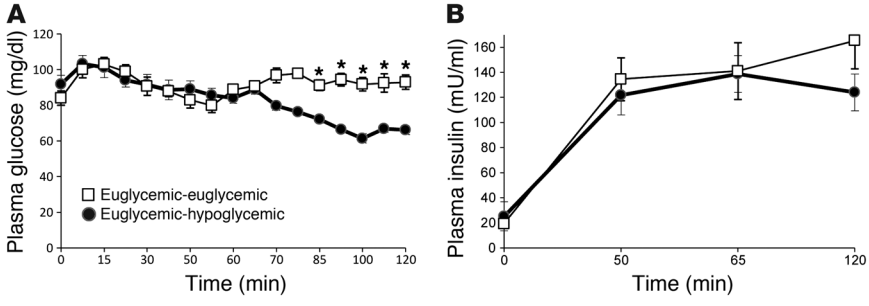

Figure 2
Plasma glucose and insulin levels. (**A**) Plasma glucose and (**B**) insulin levels (mean ± SEM) during the stepped euglycemic-hypoglycemic (black circles) and euglycemic control (white squares) study sessions. *P < 0.001 unpaired t test, euglycemic versus hypoglycemic session.

Table 1
Brain responses during euglycemia relative to hypoglycemia

Region of activation	Lat	Whole-group					Lean					Obese				
		Coordinates			Volume	*t*	Coordinates			Volume	*t*	Coordinates			Volume	*t*
		x	*y*	*z*	(mm^3)		*x*	*y*	*z*	(mm^3)		*x*	*y*	*z*	(mm^3)	
Lateral prefontal cortex																
	L	–56	7	6	534	–2.47	–	–	–	–	–	–45	24	7	12,926	–2.57
	R	39	26	9	8,460	–2.48	–	–	–	–	–	43	23	11	7,612	–2.48
Premotor cortex (BA6)																
	L	–29	–7	48	4,113	–2.63	–	–	–	–	–	–25	–2	52	11,714	–2.54
	R	54	3	20	3,499	–2.62	–	–	–	–	–	29	–3	50	14,723	–2.82
Medial prefrontal cortex																
	B	**–7**	**54**	**12**	**18,092**	**2.5**	**–2**	**56**	**12**	**15,106**	**2.68**	–	–	–	–	–
ACC																
	B	**–3**	**44**	**9**	**3,707**	**2.53**	**–4**	**45**	**8**	**1,728**	**2.38**	1	21	26	4,928	–2.48
Insula																
	L	–40	11	–3	2,818	–2.58	–	–	–	–	–	–37	14	–5	3,245	–2.66
	R	38	12	1	2,593	–2.5	37	8	2	1,114	–2.5	39	17	–3	2,385	–2.53
Striatum (caudate, putamen)																
	L	–22	7	2	3,143	–2.52	–	–	–	–	–	–18	–12	2	1,808	–2.44
	R	25	5	1	3,715	–2.65	29	1	–1	3,103	–2.46	23	4	1	4,101	–2.49
Thalamus																
	B	3	–12	8	3,425	–2.63	–	–	–	–	–	1	–14	8	6,858	–2.6
Hypothalamus																
	L	–8	–4	–6	87	–2.27	–	–	–	–	–	–8	–3	–7	125	–2.37
	R						–	–	–	–	–	5	–5	–6	174	–2.56
Hippocampus																
	L	–	–	–	–	–	**–28**	**–20**	**–15**	**1,567**	**2.5**	–	–	–	–	–
	R	–	–	–	–	–	**32**	**–18**	**–18**	**2222**	**2.54**	–	–	–	–	–
Midbrain (SN/VTA)																
	L	–	–	–	–	–	**–7**	**–19**	**–14**	**436**	**2.41**	–10	–15	–12	628	–2.58
Temporal lobe (superior/middle/inferior)																
	L	–	–	–	–	–	**–40**	**–14**	**–22**	**4,502**	**2.5**	–55	–4	–3	1,719	–2.45
	R	55	–44	12	1,580	–2.34	**41**	**3**	**–29**	**2,440**	**2.54**	41	–24	–7	1,077	–2.34
Parietal lobe (superior/middle)																
	L	–44	–39	39	9,772	–2.63	–	–	–	–	–	–40	–43	42	13,890	–2.77
	R	38	–49	43	18,216	–2.91	39	–49	44	10,418	–2.74	36	–49	45	13,210	–2.67

Note: Activity increased during euglycemia relative to hypoglycemia is indicated in bold. All other values reflect greater activity in hypoglycemia relative to euglycemia. Whole-brain FWE corrected, thresholds at $P < 0.05$. MNI coordinates were used. Lat, laterality; L, left; R, right; B, bilateral; BA, Brodmann area.

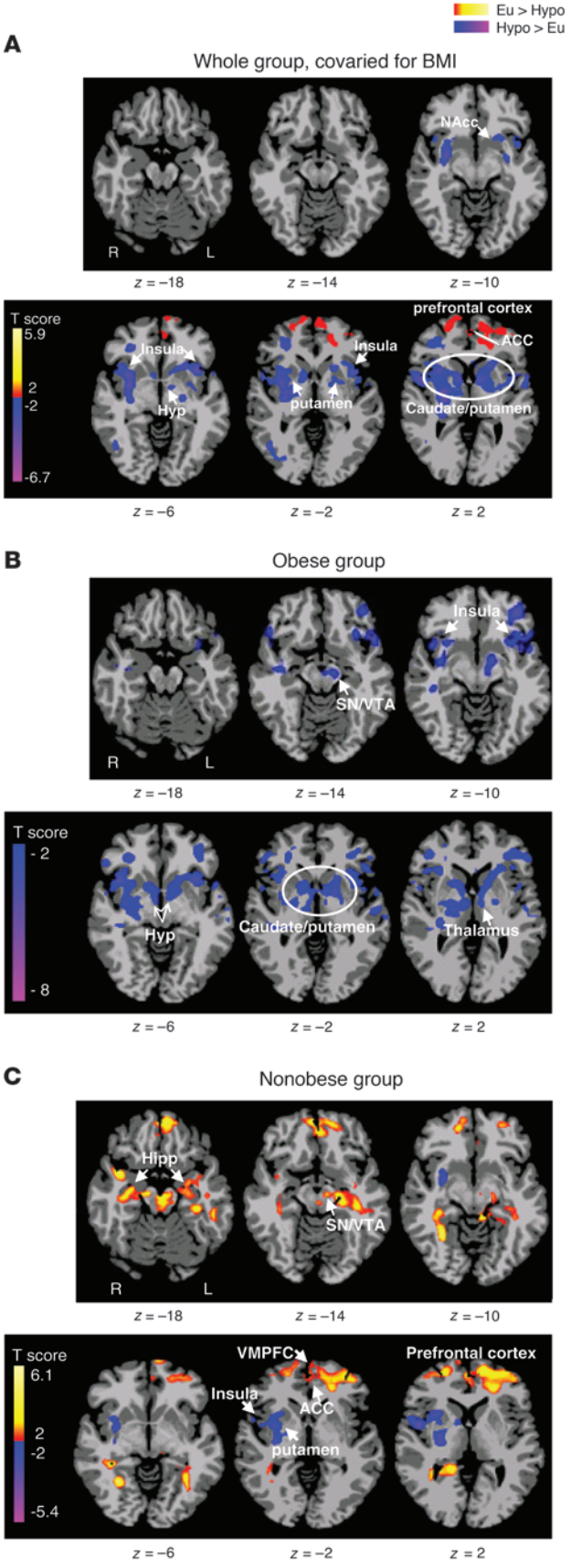

Figure 3
Differences between euglycemic and hypoglycemic conditions. Axial slices with (**A**) whole group, covaried for BMI (n = 14), (**B**) obese group (n = 5), and (**C**) nonobese group (n = 9) averages, showing brain response to euglycemia compared with mild hypoglycemia across visual cue tasks (threshold of $P < 0.05$, 2 tailed, FWE whole brain corrected). Red and yellow areas show greater activity during euglycemia, and blue areas indicate greater activity during hypoglycemia. The color scale gives the t value of the functional activity. Eu, euglycemia; Hypo, hypoglycemia; NAcc, nucleus accumbens; Hyp, hypothalamus; VMPFC, ventromedial prefrontal cortex; Hipp, hippocampus; L, left; R, right. MNI coordinates were used to define brain regions.

whereas higher levels of plasma cortisol, but not other hormones, were correlated with greater activation in reward regions, such as the insula and putamen ($P < 0.01$, corrected), in response to high-calorie food cues.

Discussion

The pattern of neural activation we observed is consistent with earlier work showing that fasting increases activation of the hypothalamus, insula, and striatum (9, 10), while meal consumption increases activation of the PFC (9). In contrast to previous work, however, we isolated one physiological stimulus, glycemic state, and demonstrated that circulating glucose levels interact with external food cues to modulate reward-related brain activation and concurrent motivation for food. Specifically, the PFC activation and decreased wanting of food during euglycemia in non-obese individuals seems to be a general response to both high- and low-calorie foods. In contrast, the stimulation of brain reward regions and motivation for food under hypoglycemic relative to euglycemic conditions is dependent on the specific type of food, since only high-calorie food cues provoked a differential brain response and greater "wanting" of food.

The role of the PFC in regulating impulse control and reducing motivation for rewarding stimuli such as food and drugs is well established (11), whereas the limbic and reward regions (e.g., insula, VTA, and striatum) promote desire and craving for rewarding stimuli (12). The thalamus acts as a relay between subcortical and cortical areas (13), and the hypothalamus is critical for fuel homeostasis and appetite control (1). Consistent with our findings, previous studies have demonstrated thalamic and hypothalamic activation under hypoglycemic conditions (14–16). The current data demonstrating oppositely directed modulation of PFC and brain reward center activation by circulating glucose support its role in stimulating executive control regions that exert inhibitory control of feeding behavior when glucose is available and promoting survival under hypoglycemic conditions by favoring instinctual motivation for food seeking and consumption when glucose is deficient.

Interestingly, BMI significantly influenced this pattern of findings. In obese individuals mild hypoglycemia (relative to euglycemia) caused activation of the VTA and bilateral subcortical hypothalamic, thalamic, insula, and striatal activation, whereas these subjects lacked the prefrontal activation seen during euglycemia relative to hypoglycemia in nonobese subjects. These results are consistent with reports showing that high BMI is associated with decreased prefrontal activity at rest (17) and after meal consumption (18) and that obese subjects have an attenuated postprandial deactivation of the hypothalamus (19). These altered obesity-asso-

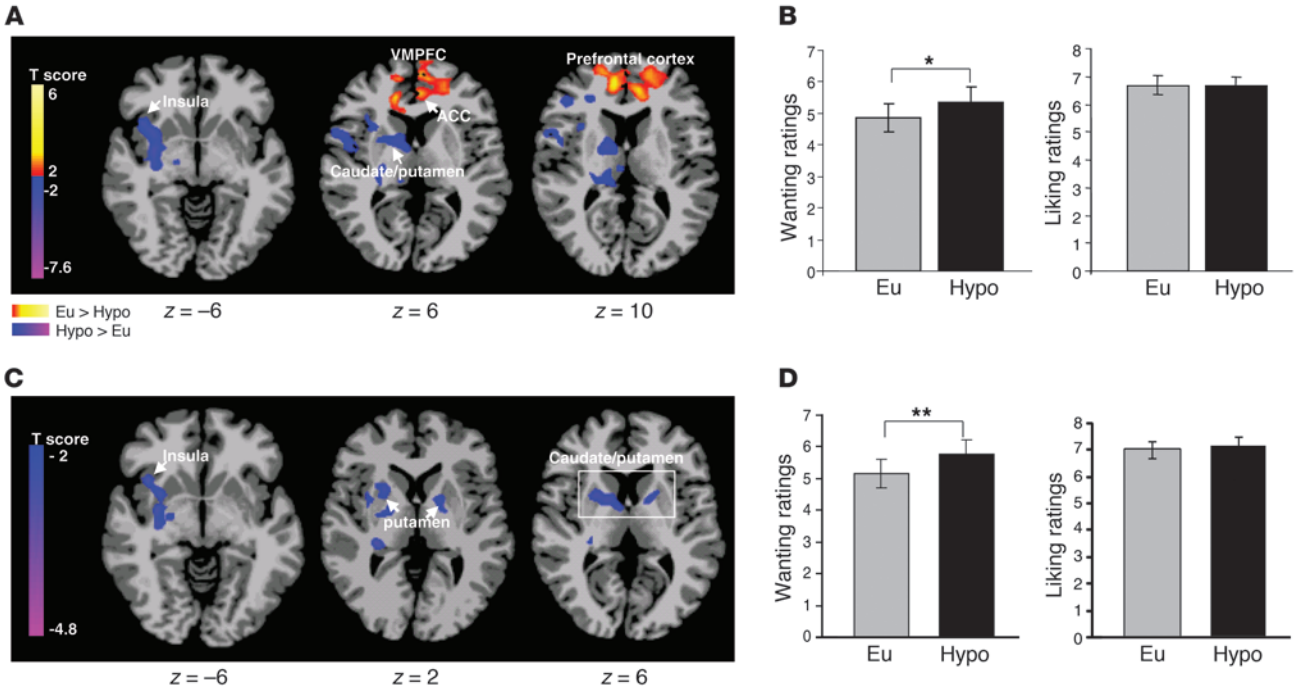

Figure 4

Condition × task effects. (**A**) Axial slices with group averages (n = 14), covaried for BMI, showing brain response to food (high-calorie and low-calorie) cues under euglycemia compared with mild hypoglycemia (threshold of $P < 0.05$, 2-tailed, FWE whole brain corrected). (**B**) Wanting and liking ratings for food during euglycemia (gray bars) and mild hypoglycemia (black bars). *$P = 0.02$. (**C**) Brain response specifically to high-calorie food images under euglycemia compared with mild hypoglycemia (threshold of $P < 0.05$, 2-tailed, FWE whole brain corrected). (**D**) Wanting and liking ratings for high-calorie foods during euglycemia (gray bars) and mild hypoglycemia (black bars); **$P = 0.006$. Red/orange areas show greater activity, and blue areas indicate more suppressed activity during euglycemia relative to hypoglycemia. MNI coordinates were used to define brain regions.

ciated neural responses to food cues may contribute to overeating behavior, especially several hours after consumption of high-carbohydrate meals, a time when glucose often declines significantly below baseline levels (3, 4).

Glucose may also influence cortical regulation of feeding behavior via its modulatory effects on midbrain neurons. Dopaminergic and GABA neurons in the VTA have projections to many brain regions, including the PFC (20), and glucose modulates GABA and dopamine release in the SN/VTA (21, 22). Hypoglycemia inhibits nigral GABA release while simultaneously increasing striatal dopamine release, suggesting disinhibition of striatal neurons (21), whereas hyperglycemia suppresses the firing of midbrain dopaminergic neurons (22). Thus, increased medial PFC activity during euglycemia relative to hypoglycemia in nonobese subjects may occur due to glucose acting on midbrain neurons and their projections to the medial PFC. On the other hand, obesity-related metabolic changes and their concomitant effects on the midbrain (SN/VTA)/medial PFC reward pathways may result in lower medial PFC brain responses, thereby putting obese individuals at greater risk for food motivation, particularly if glucose declines.

A number of peripheral hormones involved in feeding behavior, including leptin, peptide YY, and insulin, act as satiety signals and have been shown to deactivate homeostatic and hedonic brain regions (23–26). In contrast, the gut-derived orexigenic hormone ghrelin activates motivation and reward regions, including the insula and striatum, in response to food stimuli (27). In the current study we observed that mild glucose reductions engage these brain motivational centers to increase hunger and food-seeking behavior. This effect was seen in the absence of changes in circulating insulin, leptin, or ghrelin but was associated with higher levels of cortisol, which was positively correlated with activation of the insula and striatum. Behavioral studies in humans have shown that stress-induced elevations in cortisol secretion increase preference for calorie-dense foods (28), and our findings may provide a neural basis for this response.

It should be noted that we manipulated glucose levels in the presence of fixed hyperinsulinemia to investigate its effects on brain activation to visual food stimuli. Since insulin is known to inhibit feeding behavior through its actions on hypothalamic (29) and mesolimbic reward circuitry (30), our results suggest that mild hypoglycemia overcomes the inhibitory effect of hyperinsulinemia on hypothalamic and mesolimbic circuitry, promoting CNS pathways subserving food motivation and reward. How the level of insulin and insulin resistance influence the magnitude of brain and behavioral responses to food stimuli under euglycemic relative to hypoglycemic conditions requires further study.

We did not detect a specific sex-related influence on the effects of circulating glucose on brain activation to visual food cues; however, this may have been due the relatively small number of females studied. Previous imaging studies have shown sex-based differences in neural responses to food-related stimuli (31, 32) and intravenous glucose (33) as well as in the pattern of neural

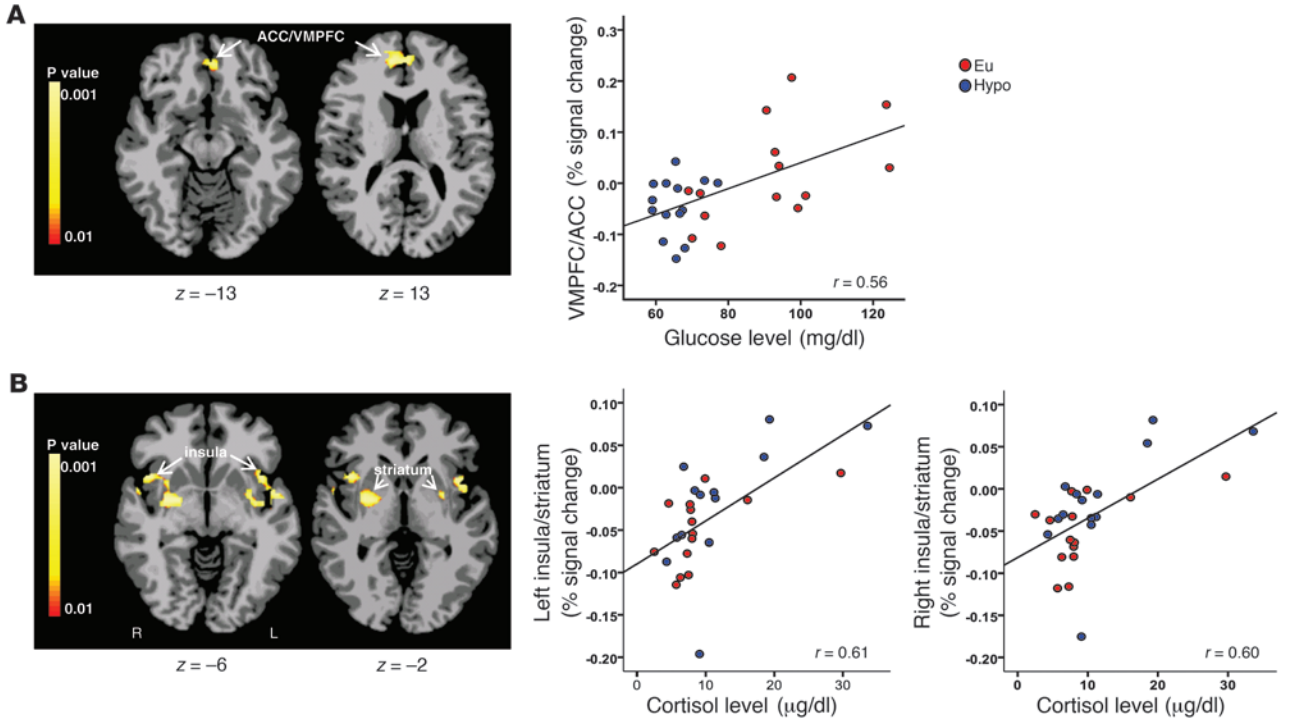

Figure 5
Whole-brain, voxel-based correlation analyses. Axial brain slices and corresponding scatter plots showing correlations between (**A**) plasma glucose levels and VMPFC/ACC response to high-calorie food images; and (**B**) plasma cortisol levels and left and right insula/striatal response to high-calorie food images. $P < 0.01$, 2-tailed, FWE whole brain corrected. Areas in yellow indicate brain regions positively correlated to plasma glucose and plasma cortisol levels. There were no outliers in these associations. MNI coordinates were used to define brain regions.

response to hunger and satiation (32, 34–36). However, no studies have investigated potential sex-based differences in the neural and behavioral response to food cues under hypoglycemia, and future work in this area is warranted.

We conclude that the glycemic state modulates the complex interplay between the PFC and hypothalamic and mesolimbic neural control of food-seeking behavior. Transient modest reductions in circulating glucose decrease prefrontal cortical inhibitory control and could promote overeating, particularly in an environment inundated with visual cues of high-calorie foods. These data imply that strategies to minimize postprandial decrements in glucose, including consumption of smaller, more frequent meals, may be helpful in reducing the risk of overeating high-calorie foods, particularly in obese individuals.

Methods

Study participants. Twenty-one healthy male (n = 12) and female (n = 9) volunteers with a mean (±SD) age of 31.4 ± 7.9 years and BMI of 25.2 ± 4 kg/m^2 who were weight stable for the 3 months before recruitment participated in this study. Fourteen subjects (9 male, 5 female; mean [±SD] age, 30.4 ± 7.9 years; BMI, 25.6 ± 4.6 kg/m^2) participated in a stepped euglycemic-hypoglycemic study; 9 of these subjects were nonobese (BMI, 22.8 ± 2.9 kg/m^2), and 5 were obese (BMI, 30.9 ± 1.4 kg/m^2). Seven subjects (3 male, 4 female; mean [±SD] age, 33.6 ± 8.0 years; BMI, 24.3 ± 2.4 kg/m^2) participated in a euglycemic-euglycemic control study. We recruited subjects with a range of BMIs that allowed us to investigate a distribution representative of the general population; however, whole group statistical analyses were covaried for BMI. All subjects participated in a screening visit, which included a medical history, physical examination, and blood tests. Female subjects were studied during the follicular phase of their menstrual cycle. We excluded individuals with a history of smoking, medical illness, hematocrit less than 33%, elevated hemoglobin A1C, claustrophobia, and metal implants, as well as vegetarians and those taking medications known to influence metabolism.

Study protocol. On the fMRI study day, subjects reported to the Yale–New Haven Hospital Research Unit at noon, where they ingested a standardized lunch. Then, an intravenous catheter was inserted into a distal arm or hand vein: this arm was gently heated, allowing for sampling of arterialized venous blood. A second intravenous catheter was established for the administration of insulin and glucose. One hour before the scanning session, participants received pre-training for the task. Subjects were given a demonstration of the two rating scales and completed a block of 15 practice trials. Subjects were informed that they would receive insulin during the study and that their glucose levels would be reduced below normal, which could lead to symptoms of low blood sugar. They were, however, blinded to the timing of changes in glycemic state.

Two hours after the standardized lunch, subjects began the 120-minute fMRI study session, which included a stepped euglycemic-hypoglycemic study or euglycemic-euglycemic control study. Blood oxygen level–dependent (BOLD) acquisitions were obtained while subjects viewed high-calorie food, low-calorie food, and non-food visual images during euglycemia and hypoglycemia. Insulin was infused at a constant rate of 2 mU/kg/min, with a variable infusion of 20% glucose adjusted to achieve euglycemia or mild hypoglycemia. This approach allowed us to examine the effects of mild hypoglycemia compared with euglycemia on brain activation and behavioral responses to food cues. Blood sampling was performed at approxi-

Table 2
Caloric density in high- and low-calorie food items used as visual food stimuli

Food item	kcal (per 100 g)
High-calorie	
Brownie	440
Cake	380
Cheeseburger	270
Chocolate	531
Cookies	450
Doughnut	400
French fries	320
Fried chicken	300
Ice cream	255
Lasagna	130
Macaroni and cheese	371
Pizza	270
Potato chips	559
Steak	250
Low-calorie	
Asparagus	22
Broccoli	35
Carrots	88
Cauliflower	93
Corn	73
Fresh fruit	90
Fruit salad	90
Peas	89
Peppers	92
Garden salad	95
Soybeans	63
Tofu	87
Tomato	94
Zucchini	95

High-calorie food items were significantly greater than low-calorie food items in caloric density (352 ± 118 vs. 79 ± 23 kcal/100 g); $P < 0.001$. The USDA National Nutrient Database was used to determine the nutritional content of food items.

mately 5-minute intervals for glucose measurements and at 10- to 20-minute intervals for measurements of plasma insulin, C-peptide, epinephrine, cortisol, glucagon, growth hormone, ghrelin, and leptin.

Visual stimuli. Tasks were presented using E-Prime software (Psychological Software Tools Inc.). Picture stimuli for fMRI consisted of high-calorie food, low-calorie food, and non-food neutral pictures. Pictures were selected from various Web sites and from the International Affective Picture System (37). High-calorie and low-calorie food pictures were balanced to ensure equivalent levels of emotional valence across glycemia sessions. All food pictures had been previously rated on affective valence in a pilot study performed outside the MRI scanner, and there was no statistical difference in affective valence between high- and low-calorie food items. Participants in the pilot study were of age and BMI similar to those of the participants in the fMRI study. High-calorie food pictures included items such as hamburgers, French fries, cookies, ice cream, chocolate, and pizza. Low-calorie food pictures included items such as salads, broccoli, bean sprouts, tofu, and fruits. High-calorie food items were significantly greater than low-calorie food items in caloric density (352 ± 118 vs. 79 ± 23 kcal/100 g) and fat content (16.6 ± 9 vs. 1.2 ± 2.5 g/100 g) ($P < 0.001$, Table 2). The USDA National Nutrient Database was used to determine the nutritional content of food items (http://www.nal.usda.gov/fnic/foodcomp/search). The control stimuli consisted of neutral, non-food pictures (e.g., building, basket, book, bicycle, and door). Non-food pictures did not include utensils, so as not to confuse participants by associating them with food stimuli. There were 8 fMRI runs, and each run included 21 randomized images of 7 high-calorie foods, 7 low-calorie foods, and 7 non-food items, resulting in a total of 168 pictures (56 high-calorie, 56 low-calorie, and 56 non-food). Each glycemic session (euglycemic and hypoglycemic) consisted of 4 runs with 84 pictures (28 high-calorie, 28 low-calorie, 28 non-food). Each picture was presented only once for a participant, and stimuli were counterbalanced and randomized across participants.

Task and behavioral ratings. A series of pictures were presented during the euglycemic and hypoglycemic phases of the task. A fast event-related design was used that included a "time-jitter" technique to effectively differentiate BOLD activity into separate events of interest within a trial (38). Each trial consisted of 3 events. First, a high-calorie food, low-calorie food, or non-food picture appeared for 6 seconds. After the picture presentation, two rating scales (liking and wanting) appeared for 3 seconds. Rating scales consisted of numbers 1–9, with a rating of 1 indicating "not at all" and a rating of 9 indicating "very much." To select their ratings, the participant pressed buttons using a non-ferromagnetic button box. At the end of a trial, a fixation cross appeared with a jittered inter-trial interval (mean, 6 seconds; range, 3–9 seconds), during which participants relaxed until the onset of the next trial. Eight runs (4 during euglycemic phase and 4 during hypoglycemic phase) were acquired, each lasting 6 minutes 36 seconds. Pictures were presented in random order and counterbalanced during each phase of the study. Each picture was presented only once for each participant.

fMRI acquisition. Images were obtained using a 3-T Siemens Trio MRI system equipped with a standard quadrature head coil, using T2*-sensitive gradient-recalled single-shot echo planar pulse sequence. Subjects were positioned in the coil, and head movements were restrained using foam pillows. Anatomical images of the functional slice locations were next obtained with spin echo imaging in the axial plane parallel to the AC-PC line with repetition time (TR) = 300 ms, echo time (TE) = 2.46 ms, bandwidth = 310 Hz/pixel, flip angle = 60°, field of view = 220 × 220 mm, matrix = 256 × 256, 32 slices with slice thickness = 4 mm and no gap. Functional BOLD signals were then acquired with a single-shot gradient echo planar imaging (EPI) sequence. Thirty-two axial slices parallel to the AC-PC line covering the whole brain were acquired with TR = 2,000 ms, TE = 25 ms, bandwidth = 2,520 Hz/pixel, flip angle = 85°, field of view = 220 × 220 mm, matrix = 64 × 64, 32 slices with slice thickness = 4 mm and no gap, 198 measurements. At the end of the functional imaging, a high-resolution 3D magnetization-prepared rapid gradient echo (MPRAGE) sequence (TR = 2530 ms; TE = 2.62 ms; bandwidth = 240 Hz/pixel; flip angle = 9°; slice thickness = 1 mm; field of view = 256 × 256 mm; matrix = 256 × 256) was used to acquire sagittal images for multi-subject registration.

fMRI analysis. All data were converted from Digital Imaging and Communication in Medicine (DICOM) format to Analyze format using XMedCon (xmedcon.sourceforge.net) (39). During the conversion process, the first 3 images at the beginning of each of the 6 functional series were discarded to enable the signal to achieve steady-state equilibrium between radio frequency pulsing and relaxation, leaving 195 measurements for analysis. Images were motion corrected for 3 translational and 3 rotational directions (40). Trials with linear motion in excess of 1.5 mm or rotation greater than 2 degrees were discarded. The first run of each phase was removed (leaving 3 runs for each phase) because some subjects had not achieved the target mild hypoglycemic level prior to the first run. Individual subject data were analyzed using a general linear model (GLM) on each voxel in the entire brain volume with 3 regressors specific for the task. The regressors were those images that pertained to the time when the subject was viewing

the high-calorie food image, low-calorie food image, or non food image. The resulting functional images for each image type were spatially smoothed with a 6-mm Gaussian kernel to account for variations in the location of activation across subjects. The output maps were normalized beta-maps, which were in the acquired space (3.44 mm × 3.44 mm × 4 mm).

To take these data into a common reference space, 3 registrations were calculated within the Yale BioImage Suite software package (http://www.bioimagesuite.org) (41, 42). The first registration performs a linear registration between the individual subject raw functional image and that subject's 2D anatomical image. The 2D anatomical image is then linearly registered to the individual's 3D anatomical image. The 3D differs from the 2D in that it has a 1 × 1 × 1–mm resolution, whereas the 2D *z*-dimension is set by slice thickness and its *x*-*y* dimensions are set by voxel size. Finally, a nonlinear registration is computed between the individual 3D anatomical image and a reference 3D image. The reference brain used was the Colin27 Brain (43), which is in Montreal Neurological Institute (MNI) space (44) and is commonly applied in SPM and other software packages. All 3 registrations were applied sequentially to the individual normalized beta-maps to bring all data into the common reference space.

Data were converted to AFNI format (ref. 45; http://afni.nimh.nih.gov) for group analysis. We applied a linear mixed effects (LME) model (condition, which was either euglycemia or hypoglycemia, by task, which was either non-food, low-calorie food, or high-calorie food images) in which the subject was treated as a random factor, covarying for BMI using the LME modeling program 3dLME from AFNI (http://afni.nimh.nih.gov/sscc/gangc/lme.html). Results were masked and converted back into ANALYZE format for viewing in BioImage Suite. Whole-brain, voxel-based correlation analyses with plasma glucose and cortisol levels were implemented using BioImageSuite (41, 42) with the application of AFNI AlphaSim family-wise error (FWE) correction for multiple comparisons. All data analyses were based on 2-tailed tests.

Biochemical analysis. Plasma glucose was measured enzymatically using glucose oxidase (YSI). Double-antibody radioimmunoassay was used to measure plasma insulin, ghrelin, leptin, and glucagon (Millipore) and cortisol (Diagnostic Products Corp.). Plasma epinephrine was measured by high-performance liquid chromatography (ESA).

Statistics. Analyses of ratings for liking, wanting, and hunger were conducted using LME models (PROC MIXED version 9.2, SAS) (46). Fixed factors in the models included session type (euglycemia or hypoglycemia), food task (non-food, low-calorie, high-calorie), and their interaction for liking and wanting ratings. For hunger ratings the model included session type and time of rating and their interaction. Post hoc linear contrasts (2-tailed 0.05 significance level) were corrected for multiple comparisons using a modified Bonferroni procedure. A random subject effect was included to account for the correlation of repeated assessments from each subject. All analyses were adjusted for BMI. Residual analysis was performed to confirm that outcomes did not depart from the assumption of normality. Paired *t* tests were performed on hormonal data averaged across euglycemia and hypoglycemia. A *P* value less than 0.05 was considered significant. Unless otherwise stated, data are presented as mean ± SEM.

Study approval. All participants provided informed consent prior to participation in this study. All aspects of the study were approved by the Human Investigation Committee at the Yale School of Medicine, New Haven, Connecticut, USA.

Acknowledgments

We thank Ellen Hintz, Anne O'Connor, Darlene Tempesta, Karen Martin, Hedy Sarofin, Terry Hickey, Kristen A. Tsou, Mikhail Smolgovsky, Ralph Jacob, Codruta Todeasa, and Aida Groszmann for their assistance, as well as the subjects who participated in this study. This work was supported by in part by grants from the NIH (DK 20495, P30 DK 45735, T32 DA022975, T32 DK07058), the NIH Common Fund (UL1-DE019586, PL1-DA024859), the Yale Center for Clinical Investigation supported by Clinical and Translational Science Award grant UL1 RR024139, and the Yale Stress Center.

Received for publication March 4, 2011, and accepted in revised form July 27, 2011.

Address correspondence to: Robert S. Sherwin, C.N.H. Long Professor of Medicine, Director, Yale Center for Clinical Investigation, Yale School of Medicine, The Anlyan Center S141, PO Box 208020 New Haven, Connecticut 06520-8020, USA. Phone: 203.785.4183; Fax: 203.737.5558; E-mail: robert.sherwin@yale.edu.

1. Marty N, Dallaporta M, Thorens B. Brain glucose sensing, counterregulation, and energy homeostasis. *Physiology (Bethesda)*. 2007;22(4):241–251.
2. Levin BE, Routh VH, Kang L, Sanders NM, Dunn-Meynell AA. Neuronal glucosensing: what do we know after 50 years? *Diabetes*. 2004; 53(10):2521–2528.
3. Melanson KJ Westerterp-Plantenga MS, Saris WH Smith FJ, Campfield LA. Blood glucose patterns and appetite in time-blinded humans: carbohydrate versus fat. *Am J Physiol*. 1999;277(2 pt 2):R337–R345.
4. Chaput JP, Tremblay A. The glucostatic theory of appetite control and the risk of obesity and diabetes. *Int J Obes (Lond)*. 2009;33(1):46–53.
5. Thompson DA, Campbell RG. Hunger in humans induced by 2-deoxy-D-glucose: glucoprivic control of taste preference and food intake. *Science*. 1977;198(4321):1065–1068.
6. Dewan S, Gillett A, Mugarza JA, Dovey TM, Halford JC, Wilding JP. Effects of insulin-induced hypoglycaemia on energy intake and food choice at a subsequent test meal. *Diabetes Metab Res Rev*. 2004; 20(5):405–410.
7. McCrimmon RJ, Sherwin RS. Hypoglycemia in type 1 diabetes. *Diabetes*. 2010;59(10):2333–2339.
8. Jones TW, Borg WP, Boulware SD, McCarthy G, Sherwin RS, Tamborlane WV. Enhanced adrenomedullary response and increased susceptibility to neuroglycopenia: mechanisms underlying the adverse effects of sugar ingestion in healthy children. *J Pediatr*. 1995;126(2):171–177.
9. Tataranni PA, et al. Neuroanatomical correlates of hunger and satiation in humans using positron emission tomography. *Proc Natl Acad Sci U S A*. 1999; 96(8):4569–4574.
10. Hinton EC, Parkinson JA, Holland AJ, Arana FS, Roberts AC, Owen AM. Neural contributions to the motivational control of appetite in humans. *Eur J Neurosci*. 2004;20(5):1411–1418.
11. Ridderinkhof KR, van den Wildenberg WP, Segalowitz SJ, Carter CS. Neurocognitive mechanisms of cognitive control: the role of prefrontal cortex in action selection, response inhibition, performance monitoring, and reward-based learning. *Brain Cogn*. 2004;56(2):129–140.
12. Naqvi NH, Rudrauf D, Damasio H, Bechara A. Damage to the insula disrupts addiction to cigarette smoking. *Science*. 2007;315(5811):531–534.
13. Sherman SM. The thalamus is more than just a relay. *Curr Opin Neurobiol*. 2007;17(4):417–422.
14. Page KA, Arora J, Qiu M, Relwani R, Constable RT, Sherwin RS. Small decrements in systemic glucose provoke increases in hypothalamic blood flow prior to the release of counterregulatory hormones. *Diabetes*. 2009;58(2):448–452.
15. Arbelaez AM, Powers WJ, Videen TO, Price JL, Cryer PE. Attenuation of counterregulatory responses to recurrent hypoglycemia by active thalamic inhibition: a mechanism for hypoglycemia-associated autonomic failure. *Diabetes*. 2008;57(2):470–475.
16. Teh MM, et al. Evolution and resolution of human brain perfusion responses to the stress of induced hypoglycemia. *Neuroimage*. 2010;53(2):584–592.
17. Volkow ND, et al. Inverse association between BMI and prefrontal metabolic activity in healthy adults. *Obesity (Silver Spring)*. 2009;17(1):60–65.
18. Le DS, et al. Less activation of the left dorsolateral prefrontal cortex in response to a meal: a feature of obesity. *Am J Clin Nutr*. 2006;84(4):725–731.
19. Gautier JF, et al. Differential brain responses to satiation in obese and lean men. *Diabetes*. 2000; 49(5):838–846.
20. Carr DB, Sesack SR. GABA-containing neurons in the rat ventral tegmental area project to the prefrontal cortex. *Synapse*. 2000;38(2):114–123.
21. During MJ, Leone P, Davis KE, Kerr D, Sherwin RS. Glucose modulates rat substantia nigra GABA release in vivo via ATP-sensitive potassium channels. *J Clin Invest*. 1995;95(5):2403–2408.
22. Saller CF, Chiodo LA. Glucose suppresses basal firing and haloperidol-induced increases in the firing

rate of central dopaminergic neurons. *Science*. 1980; 210(4475):1269–1271.
23. Batterham RL, et al. PYY modulation of cortical and hypothalamic brain areas predicts feeding behaviour in humans. *Nature*. 2007;450(7166):106–109.
24. Baicy K, et al. Leptin replacement alters brain response to food cues in genetically leptin-deficient adults. *Proc Natl Acad Sci U S A*. 2007;104(46):18276–18279.
25. Rosenbaum M, Sy M, Pavlovich K, Leibel RL, Hirsch J. Leptin reverses weight loss-induced changes in regional neural activity responses to visual food stimuli. *J Clin Invest*. 2008;118(7):2583–2591.
26. Guthoff M, et al. Insulin modulates food-related activity in the central nervous system. *J Clin Endocrinol Metab*. 2010;95(2):748–755.
27. Malik S, McGlone F, Bedrossian D, Dagher A. Ghrelin modulates brain activity in areas that control appetitive behavior. *Cell Metab*. 2008;7(5):400–409.
28. Epel E, Lapidus R, McEwen B, Brownell K. Stress may add bite to appetite in women: a laboratory study of stress-induced cortisol and eating behavior. *Psychoneuroendocrinology*. 2001;26(1):37–49.
29. Figlewicz DP, Sipols AJ. Energy regulatory signals and food reward. *Pharmacol Biochem Behav*. 2010; 97(1):15–24.
30. Figlewicz DP, Bennett JL, Aliakbari S, Zavosh A, Sipols AJ. Insulin acts at different CNS sites to decrease acute sucrose intake and sucrose self-administration in rats. *Am J Physiol Regul Integr Comp Physiol*. 2008;295(2):R388–R394.
31. Cornier MA, Salzberg AK, Endly DC, Bessesen DH, Tregellas JR. Sex-based differences in the behavioral and neuronal responses to food. *Physiol Behav*. 2010;99(4):538–543.
32. Uher R, Treasure J, Heining M, Brammer MJ, Campbell IC. Cerebral processing of food-related stimuli: effects of fasting and gender. *Behav Brain Res*. 2006;169(1):111–119.
33. Haltia LT, et al. Effects of intravenous glucose on dopaminergic function in the human brain in vivo. *Synapse*. 2007;61(9):748–756.
34. Wang GJ, et al. Evidence of gender differences in the ability to inhibit brain activation elicited by food stimulation. *Proc Natl Acad Sci U S A*. 2009; 106(4):1249–1254.
35. Smeets PA, de Graaf C, Stafleu A, van Osch MJ, Nievelstein RA, van der Grond J. Effect of satiety on brain activation during chocolate tasting in men and women. *Am J Clin Nutr*. 2006;83(6):1297–1305.
36. Del Parigi A, et al. Sex differences in the human brain's response to hunger and satiation. *Am J Clin Nutr*. 2002;75(6):1017–1022.
37. Lang PJ, Bradley MM, Cuthbert BN, eds. *International Affective Picture System (Iaps): Technical Manual And Affective Ratings*. Gainesville, Florida, USA: University of Florida, Center for Research in Psychophysiology; 1999.
38. Dale AM. Optimal experimental design for event-related fMRI. *Hum Brain Mapp*. 1999;8(2–3):109–114.
39. Nolf E. XMedCon — an open-source medical image conversion toolkit. *Eur J Nucl Med*. 2003; 30(suppl 2):S246.
40. Friston KJ, Williams S, Howard R, Frackowiak RS, Turner R. Movement-related effects in fMRI time-series. *Magn Reson Med*. 1996;35(3):346–355.
41. Duncan JS, Papademetris X, Yang J, Jackowski M, Zeng X, Staib LH. Geometric strategies for neuroanatomic analysis from MRI. *Neuroimage*. 2004; 23(suppl 1):S34–S45.
42. Papademetris X, Jackowski M, Rajeevan N, Constable RT, Staib LH. BioImage Suite: An integrated medical image analysis suite, Section of Bioimaging Sciences, Department of Diagnostic Radiology, Yale School of Medicine. Bioimage Suite. http://www.bioimagesuite.org. Accessed July 28, 2011.
43. Holmes CJ, Hoge R, Collins L, Woods R, Toga AW, Evans AC. Enhancement of MR images using registration for signal averaging. *J Comput Assist Tomogr*. 1998;22(2):324–333.
44. Evans AC, Collins DL, Mills SR, Brown ED, Kelly RL, Peters TM. 3D statistical neuroanatomical models from 305 MRI volumes. In *Nuclear Science Symposium and Medical Imaging Conference*. San Francisco, USA; 1993:1813–1817.
45. Cox RW. AFNI: software for analysis and visualization of functional magnetic resonance neuroimages. *Comput Biomed Res*. 1996;29(3):162–173.
46. Brown H, Prescott R. *Applied Mixed Models in Medicine*. Chichester, United Kingdom: John Wiley and Sons; 1999.